*32nd EPS Conference on Plasma Phys. Tarragona, 27 June - 1 July 2005 ECA Vol.**29C**, P-4.080 (2005)*

Progress of the CTS Diagnostics on TEXTOR and ASDEX Upgrade

F.Meo[1], H.Bindslev[1], J.A.Hoekzema[3], S.B.Korsholm[1,2], F.Leuterer[4], P.K.Michelsen[1], S.Michelsen[1,2], S.K.Nielsen[1], E.L.Tsakadze[1], E.Westerhof[5], P.Woskov[2], and the ECRH teams at FOM-Institute for Plasma Physics and Max-Planck-Institut für Plasmaphysik

1. Association EURATOM-Risø National Laboratory, DK-4000 Roskilde, Denmark
2. MIT Plasma Science and Fusion Center, Cambridge, MA 0213,USA
3. Association EURATOM-Forschungszentrum Jülich GmbH, Institut für Plasmaphysik, Trilateral Euregio Cluster, D-52428 Jülich, Germany
4. Max-Planck-Institut für Plasmaphysik, EURATOM Association, Garching, Germany
5. FOM-Institute for Plasma Physics Rijnhuizen, Association EURATOM-FOM, Trilateral Euregio Cluster, The Netherlands, www.rijnh.nl

Introduction: Collective Thompson Scattering (CTS) utilises the scattering of a probing radiation on the electron density to provide time resolved, spatially localized measurements of the 1-D velocity distribution of the confined fast ions in a given direction determined by the chosen scattering geometry. Different scattering geometries permit spatial scans and the resolution of anisotropy in the ion velocity distribution, which is important in fast ion physics. It has already been shown from experiments on TEXTOR that the dynamics of fast ions at sawteeth is strongly dependent on the pitch angle their orbits make with the ambient magnetic field [1]. Two CTS systems are presently installed on ASDEX Upgrade and TEXTOR. Both systems use mm-waves generated by gyrotrons as probing radiation (at 105 GHz and 110 Ghz, respectively) and measure back-scattered radiation with heterodyne receivers with 50 and 42 channels respectively. The steerable antennas on both systems allow different scattering geometries capable of measuring the fast ion distribution parallel and perpendicular to the magnetic field at different radial locations. A description of the hardware is given in reference 2.

Diagnostic capability of CTS on ASDEX Upgrade (CTS-AUG): The CTS-AUG will make use of the one of the ECRH transmission line and antenna described in Ref 3. (ECRH Antenna & transmission line #1 as probe and #2 as receiver). The choice of scattering geometry determines to a large extent the spatial resolution, robustness and resolving power, L. The resolving power is a measure of the accuracy with which the system can estimate the fast ion velocity distribution for a given velocity space resolution. For example, L = 4 corresponds to requiring that the systems resolve at least $L^2 = 16$ orthogonal components of

the fast ion distribution (essentially 16 points in the distribution) with an uncertainty, σ, smaller than the target accuracy. For this study the target accuracy is the expected phase space density 2.0×11 s m^{-4} that corresponds to 200 keV deuterium atoms. The resolving power, L, is directly proportional to beam overlap and to the probe radiation power.

.

ECE：For the system at ASDEX Upgrade, the spectral range centred on 105 GHz, the frequency of the probing radiation, the ECE has a minimum when the central magnetic field is near 2.5 Tesla. In this scenario, the fundamental electron cyclotron resonance is outside the plasma on the high field side, while the second harmonic is outside on the low field side. The result is a minimum in the ECE spectrum, the residual emission being due either to a high energy tail population, emitting into the spectral range via deeply relativistic Doppler shifts, or due to a low temperature plasma outside the last closed flux surface. Ray-trace calculations assuming Maxwellian velocity distributions and a central electron temperature of 10 keV are calculated. We conclude that, assuming thermal electron distributions, the in band ECE will generally be less than 100 eV. Except in very low-density discharges, we do not expect non-thermal tails on the electron velocity distributions in AUG.

Refraction: It is important to investigate the robustness to refraction that varies due to sudden changes in density (such as from sawteeth activity) and due to dispersion at the spectral limits of the fast ion feature. The measurements have a spectral half width of $\delta v^s = v_\alpha k^\delta / 2\pi$ where v_α is the particle velocity. There are two criteria of robustness to refraction effects; the first is robustness of the *location* of the scattering volume where the measurement is taken, and the second is robustness to the *beam overlap* (L ∝ overlap). Figure 1 shows the resolving power divided by 4 plotted against the radial location of the scattering volume for different scattering geometries of near perpendicular 1(a) and near parallel configuration 1(b). Radial spatial resolution are the horizontal error bars that represent the flux surface extents of the scattering volumes from which 90% of the received scattered radiation comes. From figure 1(a), we can see that the radial resolution for the near perpendicular geometry is between 20 cm (center) and 10 cm (toward the edge). This is different from the 10 cm resolution quoted in the study that was done in 2002 [4]. The reason for the discrepancy is that in the 2002 study, the scattering geometry was such that the receiver was below the launching mirror (ECRH antenna 1 and 4). This was the preferred

configuration since the distance between the launcher and receiver is larger (64 cm) compared to the current configuration (23 cm) where the launcher and receiver (ECRH antenna 1 and 2) are beside each other. This shorter distance will result in longer scattering volumes. However the current configuration does have one advantage of facilitating finding overlap during the experiments by utilizing the fast vertical sweeping capability of the ECRH antenna during the discharge. As we can see from the figure 1(a), the overlap and the radial displacement are robust even against density changes of 30% and also against refraction (not shown in graph) for the near perpendicular geometry. Similar results were also found for higher densities up to 8×10^{19} m^{-3}. Figure 1(b) shows the same study for the near parallel configuration. The radial spatial resolution is below 1 cm. However, this configuration is more sensitive to refraction. A 30% change in density, the radial displacements are about 10 cm on the HFS and the centre and about 20 cm on the LFS. Similar results were also found for refraction studies. It is important to note that this configuration is the worst-case scenario where there is a trade off between robustness to refraction and to more parallel configurations. The robustness can be further optimized under different scattering geometries.

Preliminary results from CTS at TEXTOR (CTS-TEXTOR): First scattering results were obtained from the upgraded CTS-TEXTOR. Figure 2 shows the spectral power density of the scattered radiation measure for two geometries during NBI heating. The figure clearly shows the asymmetry of the scattered spectral power density at higher $\phi = \angle(k^{\delta}, B)$. Not shown are the measurements during the slowing down phase after NBI switch off. Results of the slowing down rate compared to Fokker Planck simulations are found in reference 5. A spurious free spectrum is essential in the CTS experiments. Therefore it was necessary to tune of the gyrotron by modifying the magnet coil, beam voltage, and cathode coil. For the TEXTOR 110 GHz gyrotron, this usually meant a trade off of output power. The frequency spectrum of the gyrotron was also monitored during a discharge by heterodyning down the signal from a pickoff horn. Results have shown that the gyrotron during the discharge changes between 15-20 MHz most probably due to thermal effects. However, this chirping is very reproducible from shot to shot. Therefore comparing the velocity distributions from two discharges, one at a near perpendicular and one from a near parallel, we can principle have information on the bulk rotation. This currently is under investigation.

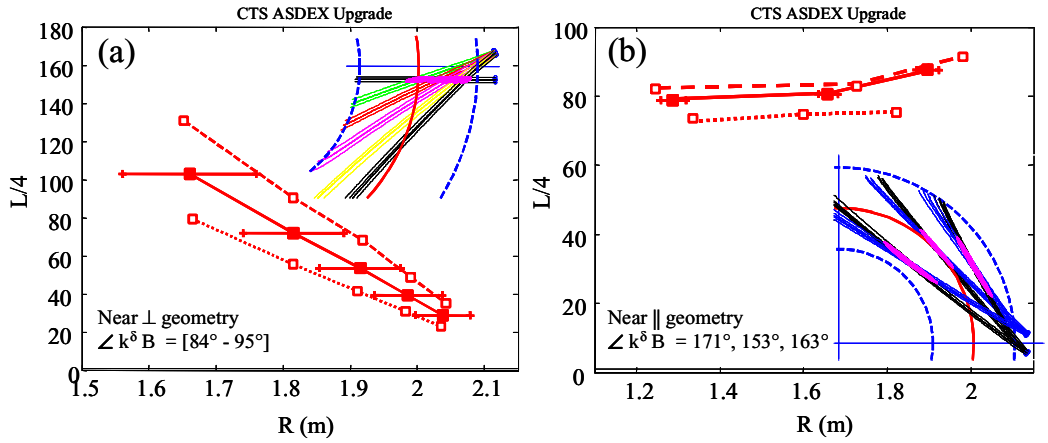

Figure 1. Resolving power, L/4, for different scattering geometries plotted against the radial location of the scattering volume. Probe launch beam is black. The dashed and dotted lines are the results of +/-30% changes in the density. P_{probe} = 500 kW, $n_e(0) = 5 \times 10$ 19 m^{-3}, $T_e(0)$ = 6 keV, T_{noise} = 100 eV, (a) Near perpendicular scattering geometry, (b) Near parallel geometry. The inserted figure shows the top view of the configuration.

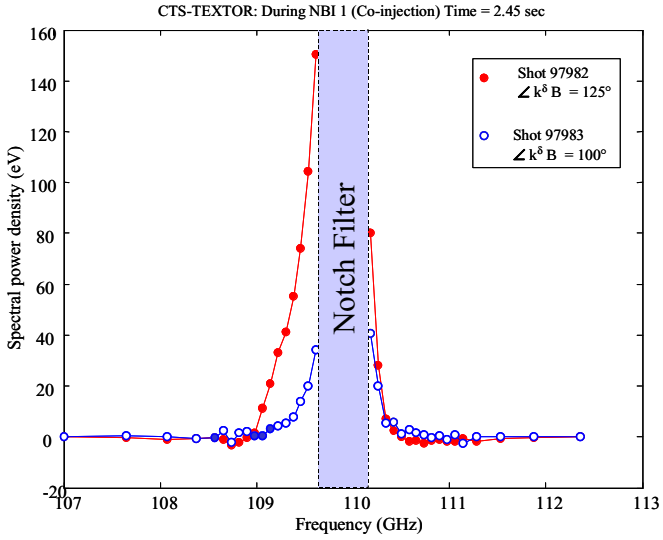

Figure 2. Spectral power density of the scattered radiation during 1.3 MW of NBI for two geometries, $\angle(\mathbf{k}^{\delta}, B) = 100°$ and 125°. $n_e(0)$ 4.0×10^{-19} m^{-3}. Power of gyrotron is 70 kW

References

[1] H. Bindslev, J. A. Hoekzema, J. Egedal, J. A. Fessey, T. P. Hughes, and J. S. Machuzak, Physical Review Letters 83, 3206 (1999).

[2] M. Michelsen et al, Rev. Sci. Instrum., Vol. 75, No. 10, Part II, October 2004

[3] F. Leuterer et al, Proceedngs of the IAEA Technical Meeting on ECRH Physics and Technology for ITER in Kloster Seeon Germany, July 2003, www.ipp.mpg.de/tmseeon/

[4] H. Bindslev, Application for Preferential Support, Fast Ion Collective Thomson Scattering diagnostic at ASDEX Upgrade, January 2002

[5] S. K. Nielsen et al, these proceedings